Journal of The Electrochemical Society, 2021 **168** 110501

Degradation-Safety Analytics in Lithium-Ion Cells and Modules: Part III. Aging and Safety of Pouch Format Cells

Daniel Juarez-Robles,[1,2,*] Saad Azam,[1,] Judith A. Jeevarajan,[1,*,z] and Partha P. Mukherjee[2,*,z]**

[1]*Electrochemical Safety Research Institute, Underwriters Laboratories Inc., Northbrook, Illinois 60062, United States of America*
[2]*School of Mechanical Engineering, Purdue University, West Lafayette, Indiana 47907, United States of America*

Owing to their versatility in cell formats, lithium-ion cells are widely used in energy storage systems. The pouch format cell architecture allows easy adaptability to a manufacturer's application needs. This study aims to characterize the interplay between cycle life aging and off-nominal conditions. Single pouch cells aged to different capacity fade (CF) levels and modules aged to 20% CF were subjected to overcharge tests. Fresh cells and fresh and aged modules were subjected to external short tests. Under overcharge conditions, fresh cells experienced thermal runaway under 1C overcharge but exhibited only swelling under C/3. Overcharged cells with 10% CF experienced swelling and thermal runaway, while cells with over 15% CF experienced swelling and venting through pouch sidewall rupture. It can be conjectured that cells with over 15% CF did not experience thermal runaway due to the relative loss of active material. Under external short, single cells exhibited slight swelling, charring of the anode tab and crumbling of the cathode. Fresh and aged modules subjected to C/3 overcharge experienced catastrophic thermal runaway. Although aging slightly delays the onset of thermal runaway, the fresh module went into catastrophic thermal runaway under external short, whereas the aged one did not.

 [DOI: 10.1149/1945-7111/ac30af]

Manuscript submitted September 10, 2021; revised manuscript received October 12, 2021. Published November 2, 2021.

The benefits of the lithium-ion technology for energy storage applications have been overshadowed by isolated but still highly publicized accidents.[1] Considerable efforts have been made to understand the behavior during the failure of these electrochemical systems.[2] Off-nominal abuse tests allow elucidating the failure mechanisms in a controlled way. Two common off-nominal scenarios experienced by lithium-ion cells in the field are overcharge and external short-circuit. They force the cell to operate outside of the safe operating conditions generating heat within it. If these two off-nominal conditions are not controlled effectively in cells or batteries, thermal runaway and fire can occur.[3,4]

The initial set of off-nominal studies was carried out on cylindrical cells that are designed with protective devices inside the cell header. The purpose and response of these devices in cylindrical cells, under off-nominal conditions, was extensively discussed in Part I and II of this work.[5,6] Unlike cylindrical cells, pouch cells are not designed with safety protection devices inside the cell. Devices used to protect against reaching high voltages (overcharge) or experiencing high currents (external short) are typically included externally on printed circuit boards (PCBs). Another difference between cylindrical cells and pouch cells is size standardization. While cylindrical cells are made based on specific measurements, pouch cells can adapt their dimensions and volume according to the application requirements. When a pouch cell is subjected to an off-nominal condition, the cells tend to noticeably expand due to high internal temperature and pressure.[7,8] Pouch format cells burst open at very low pressures (~50 psi) and when the liquid electrolyte and vapors fall on the hot surface of the pouch, they ignite and experience a fire.

External short test.—An external short circuit test can be intentionally induced by getting the cell terminals in direct contact with each other or a low impedance load, also referred to as a hard short circuit. When the low impedance external load is applied to the cell, heat is internally generated at a rapid rate due to the Joule heating effect associated with the ionic resistance.[9] Studies can be found in the literature that have focused on the lithium-ion cell or batteries' response to external short circuits, which can occur due to faulty packaging,[10] faulty wiring, or careless handling of cells.[11] Larsson et al. externally shorted fresh and aged cells with cylindrical and pouch cell architectures.[12] Swelling and burning of the cell tabs were found on the pouch cell after the test. However, the cells did not go into thermal runaway.

Wu et al. achieved results similar to Larsson et al. when an external short-circuit test was carried out on prismatic cells with three different separators and a capacity of 750 mAh.[13] Fresh and aged cells, cycled 10 and 200 cycles, were shorted with an external resistance of 30 mΩ. The current peaked instantaneously to 25 A and then dropped to less than 1 A. The temperature steadily increased to a maximum of 110 °C. The results were identical for all the three separators tested, and the number of cycles had a negligible effect on the behavior because the capacity fade was not high enough.

Overcharge test.—An overcharge condition occurs when a lithium-ion cell or battery is charged beyond the safe upper voltage limit recommended by the manufacturer. This off-nominal scenario can be induced when the wrong charger is used, due to malfunction of the charger, or due to incorrect design or malfunction of the battery management system (BMS).[2] As the cell voltage increases, the cathode is extremely delithiated, the anode is over-lithiated, and the electrolyte is driven out of the electrochemical stability window. The excess lithiation of anode causes deposition of metallic lithium on the electrode surface that can lead to separator damage.[14] The excess delithiation of cathode causes destabilization of the active material leading to mechanical degradation or fracture and oxygen release and high temperatures.[15–17] Meanwhile, the electrolyte decomposes and leads to side reactions in the anode by thickening the solid electrolyte interphase (SEI) and producing gases by reacting with the oxygen released at the cathode.[18,19] The severity of each side reaction and degradation mechanism depends on the state of charge (or extent of overcharge), state of health, the charging rate, and operating temperature.[6,20,21] Under extreme overcharge conditions, the cell is more prone to go into thermal runaway.[22]

Xiong et al. investigated the gas evolution in pouch cells at high voltages during an extended storage period at different temperatures. Their results showed that the gases produced by the cell, due to the

*Electrochemical Society Member.
**Electrochemical Society Student Member.
[z]E-mail: Judy.Jeevarajan@ul.org; pmukherjee@purdue.edu

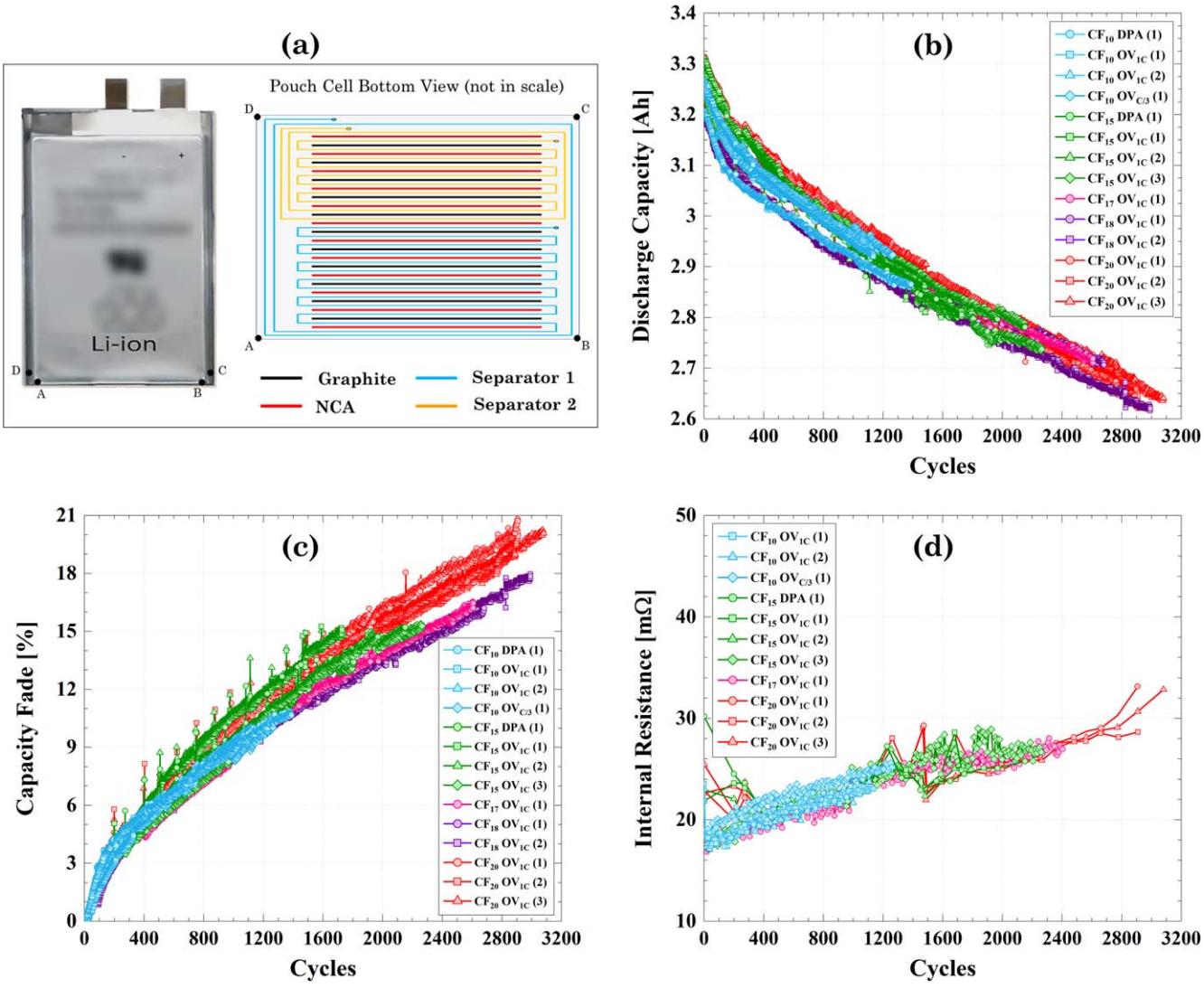

Figure 1. Cycle life aging on a graphite/NCA pouch format cell. (a) Cell photo and schematic of the internal design of the electrodes and separators; (b) discharge capacity trend, (c) capacity fade trend, and (d) internal resistance trend with cycle life aging.

high voltage, were produced on the cathode and partially consumed by the anode.[17] Sun et al. described the mechanisms of the side reactions between electrolyte solvents and the LFP cathode.[20] In their work, fresh LFP battery modules made with prismatic cells were overcharged, producing H_2, CO, CO_2, HCl, HF and SO_2. Linxiao et al. conducted a more comprehensive analysis on NMC pouch cells that were aged and overcharged.[23] They showed that CO_2 production was sensitive to high voltages, whereas hydrocarbon production was affected by aging.

Juarez et al.[16] and Klein et al.[24] investigated the effect of continuous overcharge on cycle life. Both studies demonstrated that the higher the operating voltage window is extended, the earlier the cells reach their end-of-life. The overcharge cycling condition promotes lithium metal deposition in the anode, destabilization and dissolution of the cathode transition metal, and its migration to the anode.

Current work.—The goal of this work was to determine the behavior of fresh and cycle life aged pouch format cells and modules under the two off-nominal conditions of overcharge and external short. Unlike the cylindrical cells that have protective devices embedded within the cells that protect against overvoltage, large currents (short circuits), and high temperatures, pouch cells are not designed with such devices.[5] This work aims to understand and characterize the electrochemical and thermal response of fresh and aged pouch format cells and modules under overcharge and external short conditions.

Experimental

In this study, a 3.3 Ah commercial pouch format cell was used as the test article. The pouch cell had graphite as the anode and nickel-cobalt-aluminum oxide (NCA) as the cathode active materials. The pouch cell had a design that consisted of stacked electrodes with a z-folded separator as shown in Fig. 1a. The cell had two polymeric material layers, one acting as a separator between the electrodes and one outside the anode electrode that provided additional insulation between the electrode roll and the pouch. The aging and abuse tests were carried out at ambient temperature. The aging tests on single cells and modules were conducted using two battery testers: Arbin BT200 and Arbin BTML, respectively. Thermal and electrochemical (voltage and current) data were collected at a 1 Hz sampling rate. A minimum of three cells were allocated under each protocol but in some cases as with the 15% CF, cells were allowed to age to 17% and 18% to understand where the change in off-nominal behavior occurred in the 15% CF to 20% CF range.

The modules were built using the same type of pouch format cells used in the single cell tests. The modules had a 5P5S

Table I. Summary of overcharge test conducted on fresh, and aged cells and modules.

ID	Sample	Capacity fade [%]	Cycles	Off-nominal Test	Maximum temperature [°C]	Charring	Swelling	Venting	Thermal runaway	Fire
CF_{00} OV_{1C}[1]	Single Cell	0	0	Overcharge, 1C-rate	93	No	Yes	Yes	No	No
CF_{00} OV_{1C}[2]	Single Cell	0	0	Overcharge, 1C-rate	1000	Yes	Yes	Yes	Yes	Yes
CF_{00} OV_{1C}[3]	Single Cell	0	0	Overcharge, 1C-rate	897	Yes	Yes	Yes	Yes	Yes
CF_{10} OV_{1C}[1]	Single Cell	10	1123	Overcharge, 1C-rate	360	Yes	Yes	Yes	Yes	Yes
CF_{10} OV_{1C}[2]	Single Cell	10	1136	Overcharge, 1C-rate	74	No	Yes	Yes	Yes	No
CF_{15} OV_{1C}[1]	Single Cell	15	1727	Overcharge, 1C-rate	356	Yes	Yes	Yes	Yes	Yes
CF_{17} OV_{1C}[1]	Single Cell	17	2799	Overcharge, 1C-rate	97	No	Yes	Yes	No	No
CF_{18} OV_{1C}[1]	Single Cell	18	3239	Overcharge, 1C-rate	103	No	Yes	Yes	No	No
CF_{20} OV_{1C}[1]	Single Cell	20	2907	Overcharge, 1C-rate	66	No	Yes	Yes	No	No
CF_{20} OV_{1C}[2]	Single Cell	20	2909	Overcharge, 1C-rate	53	No	Yes	Yes	No	No
CF_{20} OV_{1C}[3]	Single Cell	20	3080	Overcharge, 1C-rate	92	No	Yes	Yes	No	No
CF_{00} $OV_{C/3}$[1]	Single Cell	0	0	Overcharge, C/3-rate	47	No	Yes	Yes	No	No
CF_{00} $OV_{C/3}$[2]	Single Cell	0	0	Overcharge, C/3-rate	39	No	Yes	Yes	No	No
CF_{10} $OV_{C/3}$[1]	Single Cell	10	1265	Overcharge, C/3-rate	62	No	Yes	Yes	No	No
M_CF_{00} OV	Module	0	0	Overcharge, C/3-rate	842	Yes	Yes	Yes	Yes	Yes
M_CF_{20} OV	Module	20	2000	Overcharge, C/3-rate	875	Yes	Yes	Yes	Yes	Yes

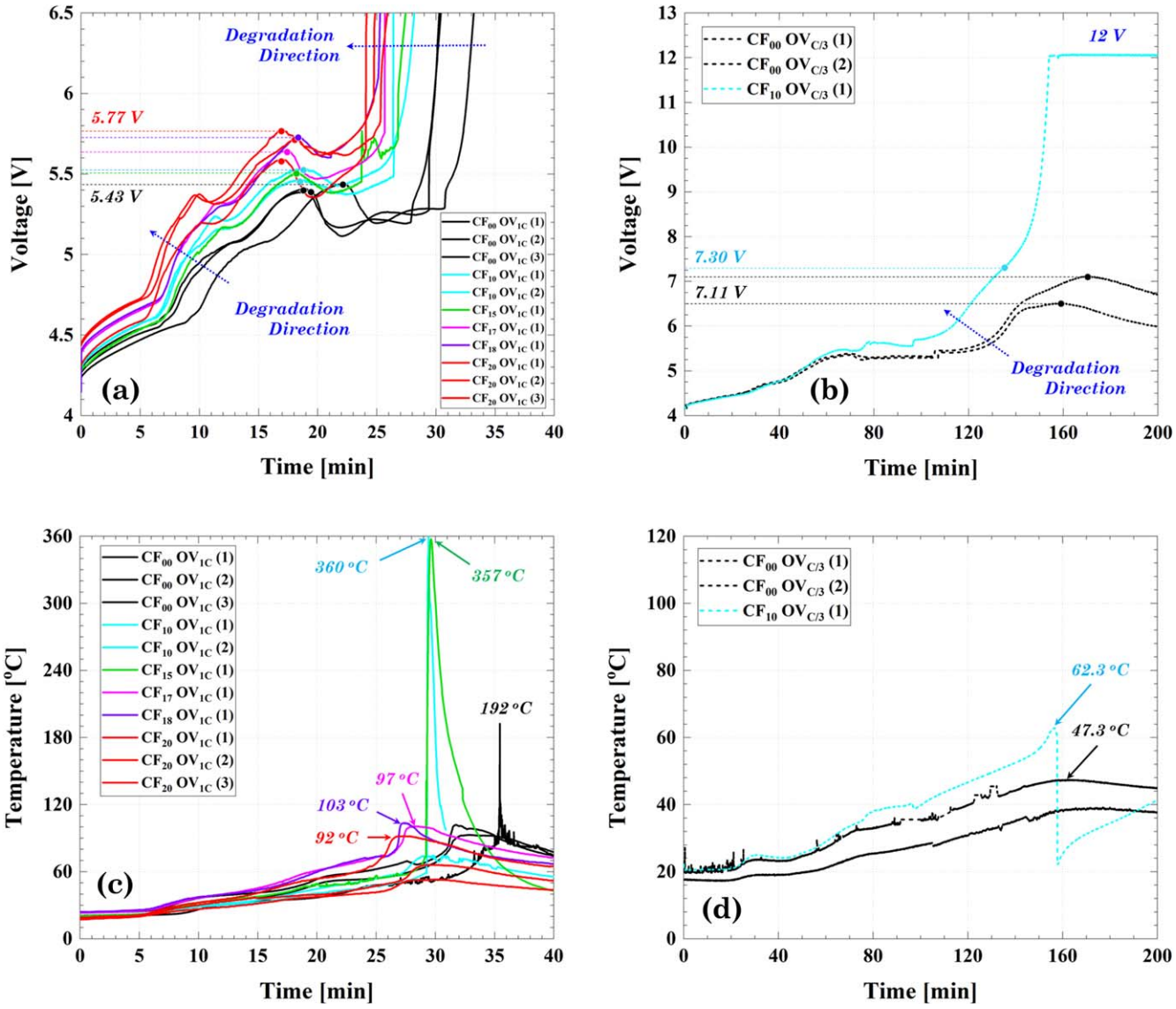

Figure 2. Voltage and temperature response comparison of overcharged cells with different capacity fades. (a) and (c) cells overcharged at 1C-rate, (b) and (d) cells overcharged at C/3-rate.

configuration (i.e., 5 cells in parallel (bank), 5 banks in series), as shown in Fig. 6a. The connection of the cells was made by using aluminum and nickel blocks. The connection was reinforced with a threaded rod and tightened with bolts. The electrical connections between the banks were performed using a cable. The base of the module consisted of an aluminum metallic block with slots aimed to provide 2 mm spacing between the five cells in each bank.[25] The module was enclosed in an acrylic frame with cut-outs to provide an enclosure that still allowed air to flow through it.

Aging test.—The manufacturer's specified voltage window for the pouch cell was 2.7 to 4.2 V. Consequently, the module voltage window was 13.5 to 21.0 V and the module capacity was 16.5 Ah. The aging test for single cells was performed as follows. Cells were charged using the CCCV protocol with a constant current charge at 1C-rate (3.3 A) up to 4.2 V and voltage held at 4.2 V until the current fell to C/20 (165 mA) value. The discharge was performed with a constant current (CC) at 1C-rate (3.3 A) to 2.7 V. A 30-min rest period was included after every charge and discharge step. The end-of-life criteria for the single cell test was defined as reaching 20% capacity fade. Cells were removed at capacity fade levels of 10%, 15%, 17%, 18%, and 20% for further analyses or tests. The aging test for modules was carried out as follows. Charging was performed using the CCCV charge at C/2-rate (1.65 A) up to 21.0 V with a C/50 (66 mA) cut-off current. The discharge was performed using a CC at C/2-rate down to 13.5 V. A 30-min rest period was provided between every charge and discharge step. Internal resistance measurements were recorded for the first discharge and after every 25 cycles. The internal resistance was calculated by applying a 1.5C pulse for 100 ms at 50% DOD during the relevant discharge step. The end-of-life criteria for the module was defined as reaching 20% capacity fade.

Overcharge test.—The manufacturer-recommended end-of-charge voltage for this pouch cell was 4.2 V. Hence, the cell was considered to be overcharged when the voltage exceeded 4.2 V. Before the overcharge abuse test, the cells were fully charged using the protocol described in the experimental section and then over-charged using 1C (3.3 A) or C/3 (1.1 A) currents to a 12 V limit for a maximum of six hours or until an off-nominal event occurred.

Similarly, the modules were fully charged using the protocol described in the experimental section prior to the overcharge test. The fully charged module was overcharged using a 5.5 A (C/3) up to a 50 V limit for a maximum of six hours or until an off-nominal

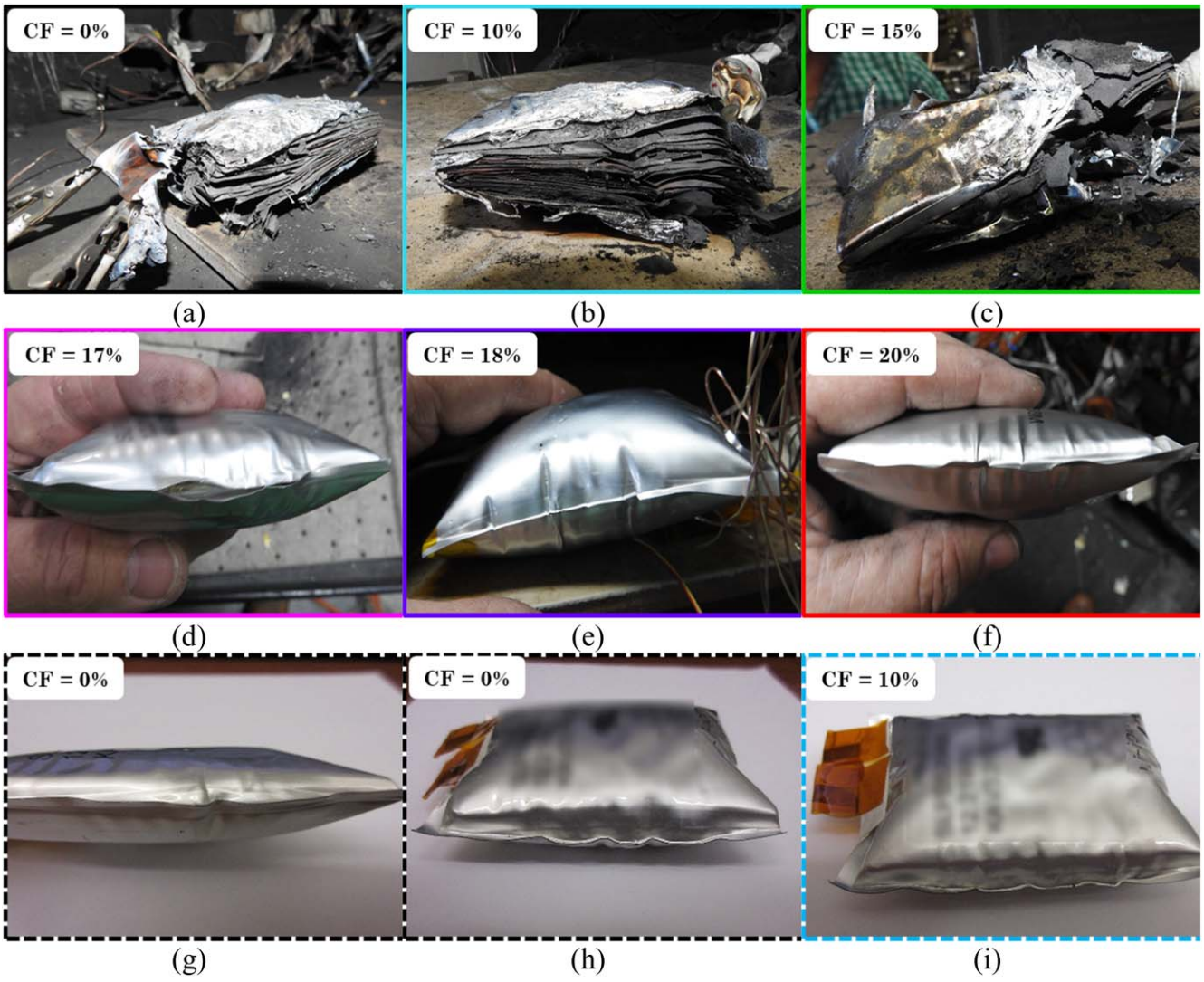

Figure 3. Effect of the charge rate on the physical response of fresh and aged cells under overcharge conditions. Cell overcharged at (a)–(f) 1C-rate; and (g)–(i) C/3-rate.

event occurred. Temperature and voltage measurements of the banks were collected along with the module voltage.

External short test.—The external short test was conducted on fully charged cells and modules with a 15 mΩ load. Low impedance external shorts are characterized by a load resistance that is equal to or less than the internal resistance of the test article.[5] The average internal resistance, at 50% SOC, of the fresh cells was 18 mΩ. The internal resistance of the aged cells was lower than 30 mΩ, Fig. 1d. For consistency, a 15 mΩ load was chosen for the short circuit test. The short circuit load was maintained for 3 h. The sampling rate for the first 3 s was 1 kHz to capture the initial current spike produced at the application of the short circuit.

Results and Discussion

Aging test in single cells.—The pouch cell design used to study the interplay between the cycle life aging and off-nominal conditions is shown in Fig. 1a. Figure 1a also provides a schematic of the design of the electrode roll and its placement in the pouch format cell. A destructive physical analysis in an inert glovebox revealed the cell had two separator pieces. The physical details and internal distribution of the electrodes and separators are relevant in the discussion of the results obtained under the off-nominal conditions.

The state of health of the cells was evaluated in terms of the discharge capacity and percentage of capacity fade as well as the changes observed with the internal resistance of the cells, Figs. 1b –1d. For a more objective comparison, capacity fade percentage was calculated by normalizing the discharge capacity curve with the highest capacity achieved during the first complete cycle. The nomenclature, $CF_XOV_{C\text{-}rate}(N)$ and $CF_XDPA(N)$, indicates that the capacity fade (CF) was X%. The off-nominal conditions are indicated as: OV for overcharge, EX for external short. DPA was used for the cells that underwent destructive physical analysis. The subscript after OV indicates the current rate for the overcharge test. The number N indicates the replicate number. Cells labeled with the letters DPA had been subjected to destructive physical analysis with samples taken for spectroscopic analysis.

The discharge capacity curves were similar for all cells indicating the consistency of the aging results (Fig. 1b). The total number of cycles for cells and modules obtained from the study are listed in Table I. Cells had completed between 1123 (CF_{10} $OV_{1C}{}^{2}$) and 1388 times (CF_{10} DPA^{1}) at 10% capacity fade. Another batch of cells gave between 1727 (CF_{15} DPA^{1}) and 2264 cycles (CF_{15} $OV_{1C}{}^{3}$) at 15% capacity fade. Cells that were cycled until 20% capacity fade had completed between 2907 (CF_{20} $OV_{1C}{}^{1}$) and 3080 (CF_{20} $OV_{1C}{}^{3}$) cycles. The number of cycles required to reach the end of life (>20% CF) of the pouch cell under this study was considerably higher than

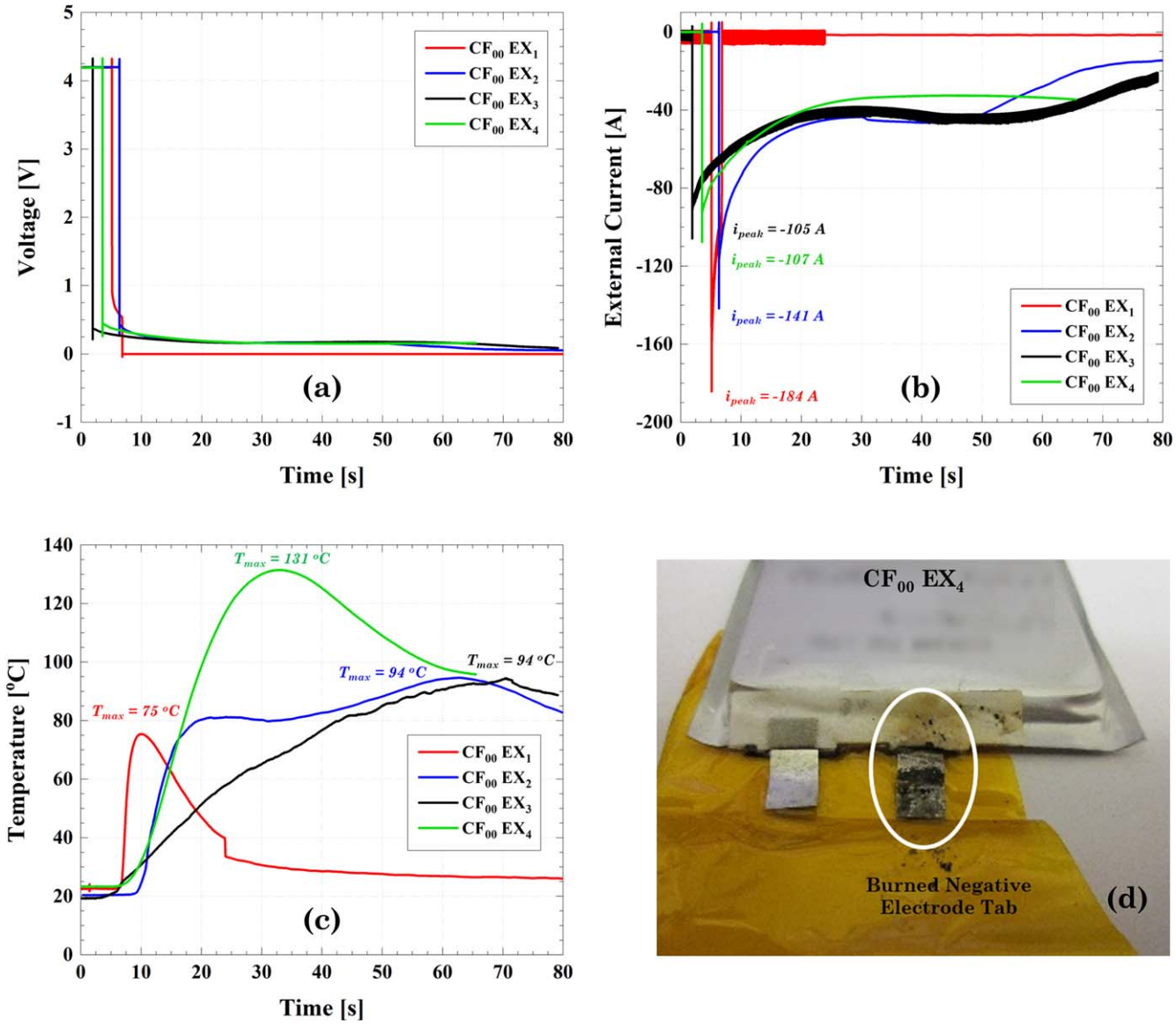

Figure 4. Voltage and temperature response comparison of externally shorted fresh cells. (a) voltage; (b) peak current recorded on imposition of the hard short; (c) cell temperature; (d) photo of cell with burned tab in externally shorted cells.

that for the cylindrical cell design that was tested in Part I of this study.[5] The capacity fade plot, Fig. 1c, shows only two of the three degradation phases proposed by Yang et al. for the capacity fade.[26,27] The first degradation phase occurred in the first 400 ∼ 500 cycles. A rapid increase in capacity fading attributed to SEI formation characterizes this phase. The second degradation phase occurred after cycle 500. The main characteristic of this phase is the linear trend in capacity fading attributed to a reduction in lithium inventory due to side reactions. These reactions lead to SEI thickening and the onset of lithium plating. The third degradation phase attributed to a rapid increase of lithium plating rate is the transition point from linear to nonlinear aging. That transition point was not apparent for the test articles studied under our test program. Destructive analysis of the aged electrodes revealed isolated silver spots on the edge of the graphite electrodes, confirming the presence of lithium plating. At the end of the cycle life, none of the cells exhibited swelling. This response indicates that the side reactions induced by cycle life aging do not produce a significant amount of gases for the pouch cell design used in this study.

The cell internal resistance, Fig. 1d, increased in value by 50% with respect to the resistance of the fresh cell, varying from 19 mΩ to 30 mΩ in a linear way throughout the aging test. The third phase of degradation proposed by Yang et al. is also characterized by an accelerated increase in impedance, or resistance, of the cell. This increase was not evident in Fig. 1d and may indicate that the cell had not reached the accelerated degradation phase.

Overcharge test in single cells.—The results for the overcharge tests of the 3.3 Ah single cells are shown in Figs. 2 and 3. Fresh and aged cells were fully charged prior to the overcharge test. During overcharge, the cell voltage and temperature increase in a non-uniform fashion driving the cell through degradation mechanisms in the anode (lithium plating) and cathode (mechanical degradation of active particle and electrode), the release of gases, and heat and finally to thermal runaway. Figure 2a shows the voltage characteristics for the overcharge test conducted using a 1C current. The results indicate that overcharged fresh cells took longer to go into thermal runaway than the aged cells that were overcharged. Cycle life aged cells have a higher internal resistance and reach the cut-off voltage (12 V) faster. The increase in internal resistance causes a greater overpotential at the time of overcharge. Therefore, the peak voltage of the aged cells observed under the overcharge condition

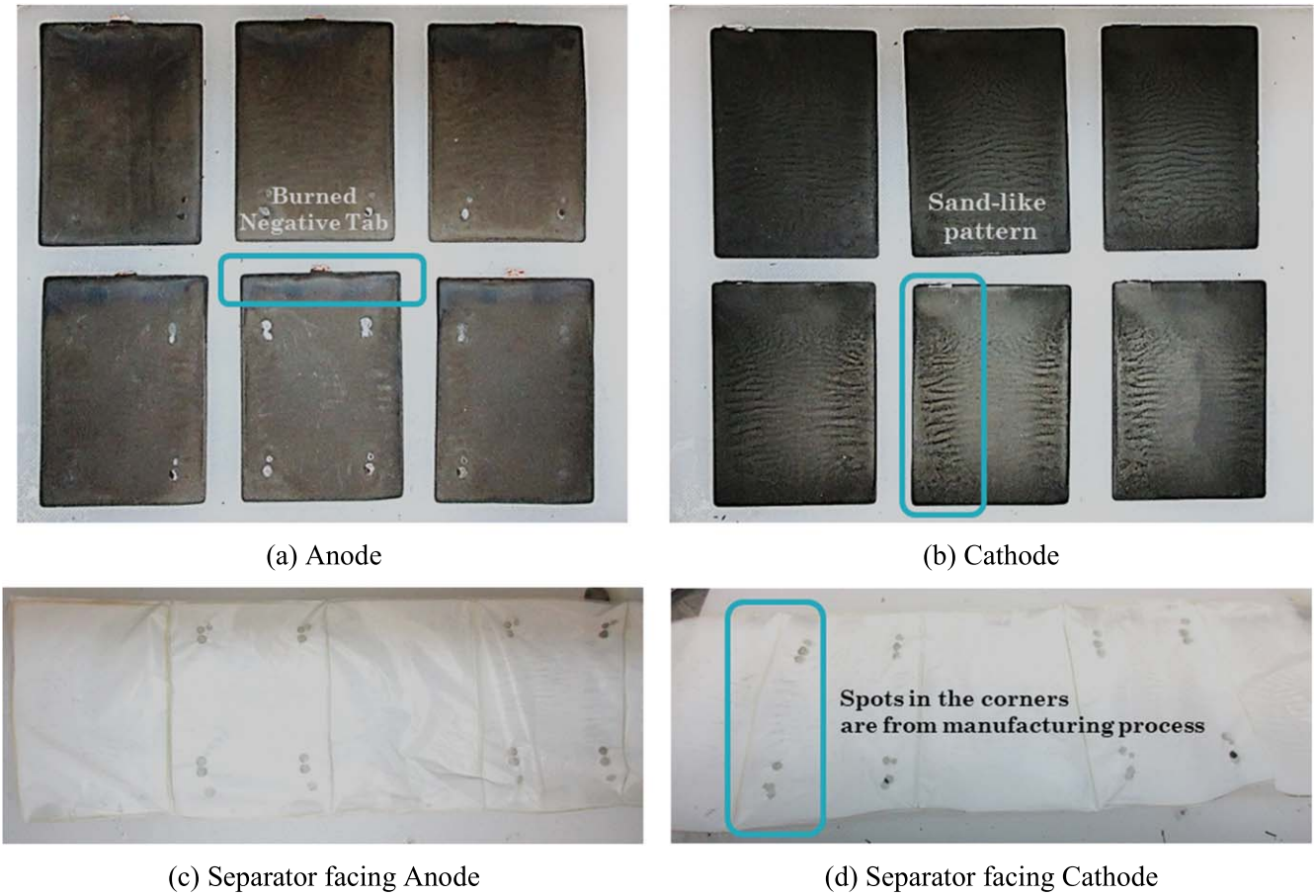

Figure 5. Post-mortem analysis of fresh externally shorted cell (CF_{00} EX[4]). Representative samples from (a) anode, (b) cathode, (c) separator facing anode, and (d) separator facing cathode.

increased before thermal runaway occurred Fig. 2a. The effect of the charging rate on the voltage response can be seen by comparing Figs. 2a and 2b. A low charge rate led to a lower overpotential and extended the off-nominal test time. Cells overcharged at C/3-rate reached a higher but more gradual voltage peak taking approximately ten times the time period to reach this voltage compared to the cells overcharged at the 1C-rate. This can be attributed to the slower changes occurring internal to the cells such as lithium dendrite formation, electrolyte degradation and temperature rise, due to the overcharge at the lower rate. Cells overcharged at the C/3 rate did not experience thermal runaway.

The thermal response of the cells, Fig. 2c, showed that fresh and aged cells up to 15% capacity fade were prone to go into thermal runaway when overcharged at a 1C rate. In particular, fresh cells went into thermal runaway during the overcharge test at 1C rate and caught fire leading to temperatures above 900 °C (see Table I and Fig. 3a). Cells with 10% and 15% CF initially exhibited some swelling and finally went into thermal runaway. Unlike fresh cells, during 1C rate overcharge, the 10 and 15% CF aged cells only reached a maximum temperature of 360 °C when thermal runaway occurred. The cells exhibited charring of the electrodes and pouch as shown in Figs. 3b and 3c. The overcharge test for the three cells with 20% CF cell, showed that the maximum temperature obtained was 92 °C. The cells only swelled due to the gases generated by the high voltage and eventually ruptured the pouch, venting the gases from the cells. No thermal runaway or fire was observed in any of the three cells. In order to figure out if there was a capacity fade threshold for thermal runaway occurrence, additional overcharge tests were conducted on 17% and 18% CF cells. The results from Figs. 2 and 3, clearly shows that the cells only swelled and vented but did not go into thermal runaway. The cell failure for these cells was due to a rupture of the pouch on the side farthest from the positive terminal, as shown in Figs. 3d to 3f, exposing the electrodes-separator assembly similar to that observed with the 20% CF cells. No visible damage was found on the tabs. Thus, 15% CF seems to be the threshold for thermal runaway under overcharge at 1C rate conditions. At this state of health, the degradation induced by aging mitigates the catastrophic effects imposed by overcharge.

For the cells overcharged at a C/3 current, Fig. 2d, the maximum temperature was 62.3 °C and was observed with the cell aged to 10% cf. The charging rate affects the overpotential and the irreversible heat generated by the cell and the degradation imposed on the cell due to the high voltage.[21] Interestingly, the cells overcharged at a C/3 current only failed by rupture of the pouch. The rupture on the same side of the pouch in all cells was due to the internal electrode roll design. The voltage and temperature drop were small during the venting and, in some cases, indistinguishable. After cell rupture, the cell voltage and temperature continued to increase. This increase in voltage makes this pouch cell design, which does not have an internal protective device, different from a cylindrical cell with a CID. The CID in the 18650-type cylindrical cell internally disconnects causing a loss in voltage whereas the voltage of the pouch cell continues to increase until it reaches the voltage limit set for the test. The generation of gases due to the reaction between the electrolyte and deposited lithium as well as the decomposition of the electrolyte experienced at the high voltages caused swelling of the cells. If the cells are not designed with an internal restraint on the flat surfaces of the electrodes, the generation of gases and the swelling causes the electrodes to move away from one another and it is also possible that the gases may be trapped between the electrodes.

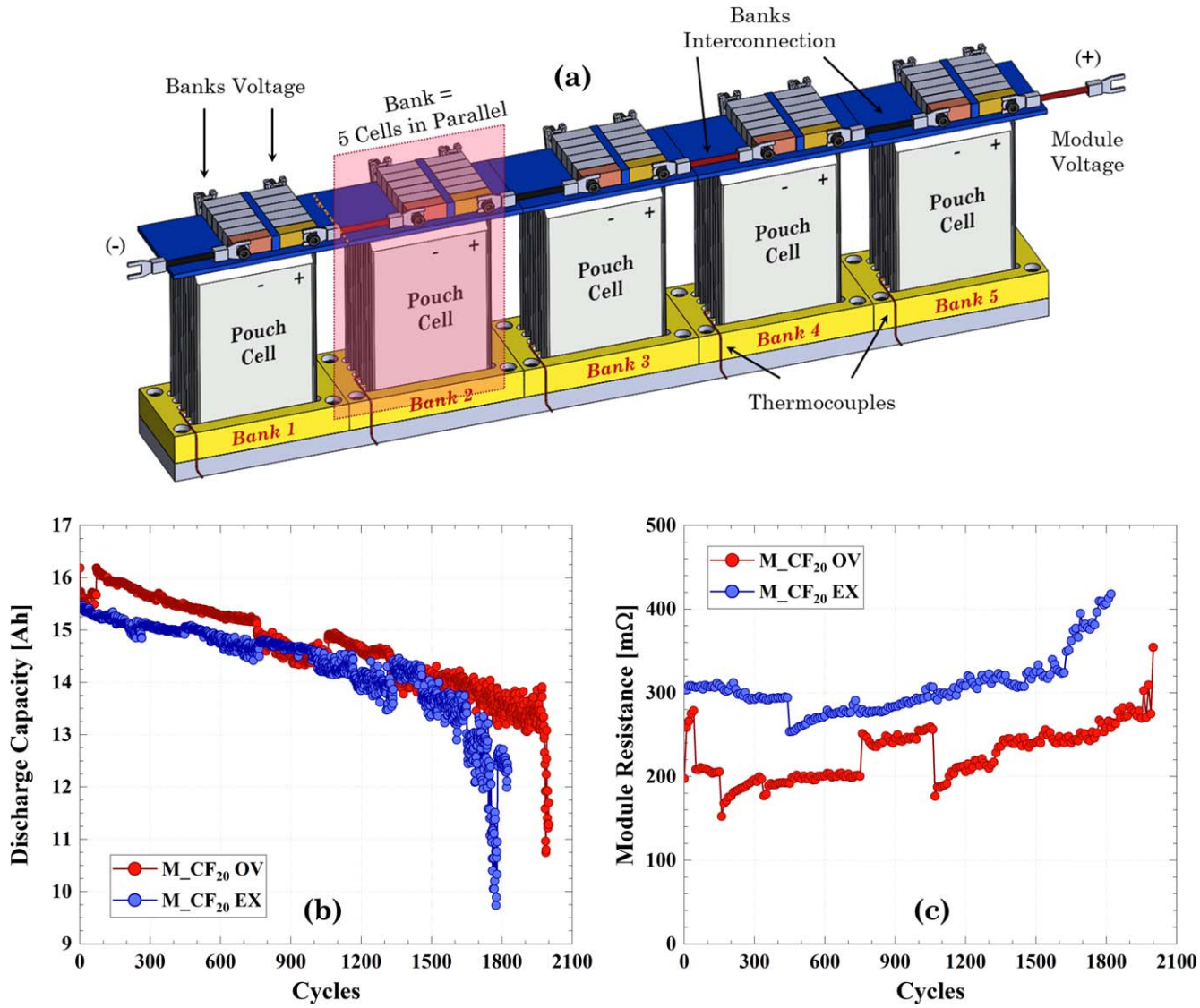

Figure 6. Cycle life aging of a 5P5S pouch cell module. (a) Schematic of the module depicting the interconnects between cells in a bank and between banks; (b) discharge capacity trend, and (c) module internal resistance trend with cycle life aging.

The movement of the electrodes hinders the lithiation and delithiation process thus causing major changes in cell capacity.

External short test in single cells.—The results of the external short test for single cells are shown in Fig. 4. Fresh cells were fully charged prior to the external short test. No external short tests were conducted on aged cells. Figure 4a shows the sudden voltage drop from 4.2 V to 0.2 V in less than 8 s. The external load resistance was connected for 3 h to characterize the temperature increase on continued short circuit load, but the significant changes in voltage and temperature happened during the first 80 s. The peak current observed at the start of the external short imposition on the cells was also measured at the rate of 1 kHz. The short circuit test on fresh cells, generated peak currents that varied between 105 A and 184 A, equivalent to approximately 32 C-rate and 56 C-rate, respectively Fig. 4b. The maximum temperature of the cells varied between 75 °C and 131 °C for the two cells discussed above, Fig. 4c. The absence of the short circuit protection internal to the cell results in a situation where neither the current nor the cell temperature can be controlled. In the case of the 18650 cylindrical cells studied in Part II, it was found that the maximum temperature generated on application of the hard short was observed for about the entire three hour period.[6] This behavior was not observed in the pouch cells under this study. Temperatures dropped after the peak temperature was attained. This might be due to the burning of the tabs in the cells that prevents the cell from seeing the short circuit load for the three-hour period.

The cell did not swell, and the only visible external damage was charring around the negative tab, see Fig. 4d. Although there was no swelling, the electrodes-separator assembly got exposed to the ambient environment through a tiny hole next to the burned tab. However, destructive analysis of the cell showed no charring around the tab inside the cell. It was also observed that the outer layer of the separator was completely stuck to the inside of the pouch, making it difficult to separate from the pouch. The electrodes were also dry and no evidence of liquid electrolyte was found on the shorted cell.

A sand-dune-like pattern was found on the surface of all the electrodes. The pattern was more evident in the positive electrode but was also present at the negative graphite electrode. The spot marks from the separator were also observed in all the electrodes. In fact, some of those spots show a cathode material detachment, as shown in the black spots from the separator facing cathode, see Fig. 5d. The pattern found on the electrodes was also found on the separator. Samples from the charred and sand-dune type areas were analyzed using SEM/EDS spectroscopic methods. The sand-dune patterns at the cathode turned out to be agglomerations of crumbled

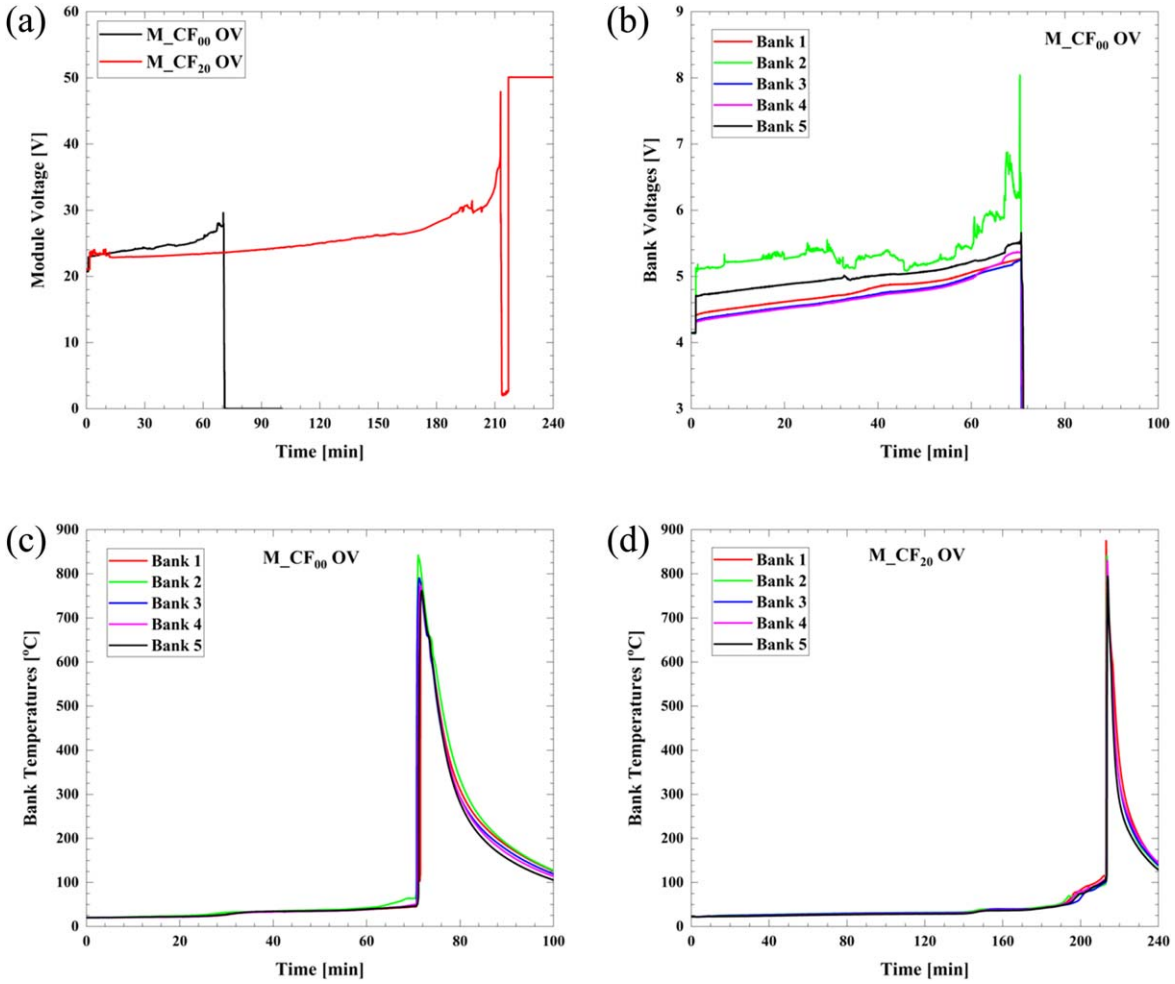

Figure 7. Overcharged test of modules: (a) Voltage comparison for fresh and cycle life aged modules. Bank voltages for (c) fresh module. Bank temperatures for (d) fresh and (e) cycled aged module.

cobalt particles and the pattern may be due to the heat produced that may have resulted in shrinkage of the binder used in the cathodes as well as shrinkage of the separator due to the heat experienced. Although the tab for the negative electrode was charred, no significant damage was found on the electrode surface.

Aging test in modules.—The cycle life aging test of the 5P5S module was carried out on a custom-made module using the pouch format cells from the same batch. The module schematic in Fig. 6a shows the connection between the cells and banks. Two modules were aged to 20% CF and the corresponding discharge capacity is shown in Fig. 6b. Unlike individual cells, the modules exhibited all three degradation phases. The first degradation phase occurred in the first 100 cycles. After 100 cycles, the degradation of the module exhibits a linear trend in the next 1500 cycles. Finally, the degradation of the module accelerates from 1700 and 1900 cycles, for the M_CF$_{20}$ EX and M_CF$_{20}$ OV modules, respectively. At 20% CF, 1826 and 2000 cycles were obtained for the M_CF$_{20}$ EX and M_CF$_{20}$ OV modules respectively. It took 1000 fewer cycles for the modules compared to the individual single cells to reach 20% cf Fluctuation observed with the discharge capacity curves was due to the absence of a battery management system (BMS). Module resistance was also measured as a state of health indicator. This parameter reflects the total resistance of the module, which includes not only the internal resistance of the cells but also on the electrical connections between the cells.

Overcharge test in modules.—The electrochemical and thermal results of the overcharge test performed on the modules are shown in Fig. 7. Figure 7a shows a comparison of the module voltage during the overcharge test. The overcharged fresh module, M_CF$_{00}$OV, failed after 70 min while the aged module, M_CF$_{20}$OV, with 20% CF failed after 210 min. Both modules failed before reaching the 50 V voltage limit set in the equipment, but it took three times longer for the aged module to go into thermal runaway. However, once the modules went into thermal runaway, the maximum temperature reached by both modules was not significantly different, with 842 °C observed in Bank 2 for the M_CF$_{00}$ OV module; and 875 °C observed in Bank 1 for the M_CF$_{20}$ OV module, see Figs. 7c and 7d. In the overcharged fresh module, Bank 2 exhibited a random behavior and was the first bank to fail followed by Bank 5, see Fig. 7b. Bank voltages were not recorded for the overcharged aged module. Both modules went into complete fire and thermal runaway, as shown in the post-test photos from Figs. 8b and 8d. For the overcharged fresh module, the pouch material for all cells got burned and exposed the charred electrodes, Fig. 8b. For the overcharged aged module, the temperature achieved during thermal runaway was such that it melted the acrylic frame that was used to as an enclosure of the cell module, Fig. 8d.

External short test in modules.—The results of the external short test carried out on the fresh and aged modules are shown in Fig. 9, and Table II. Similar to the single cells, during the external short test,

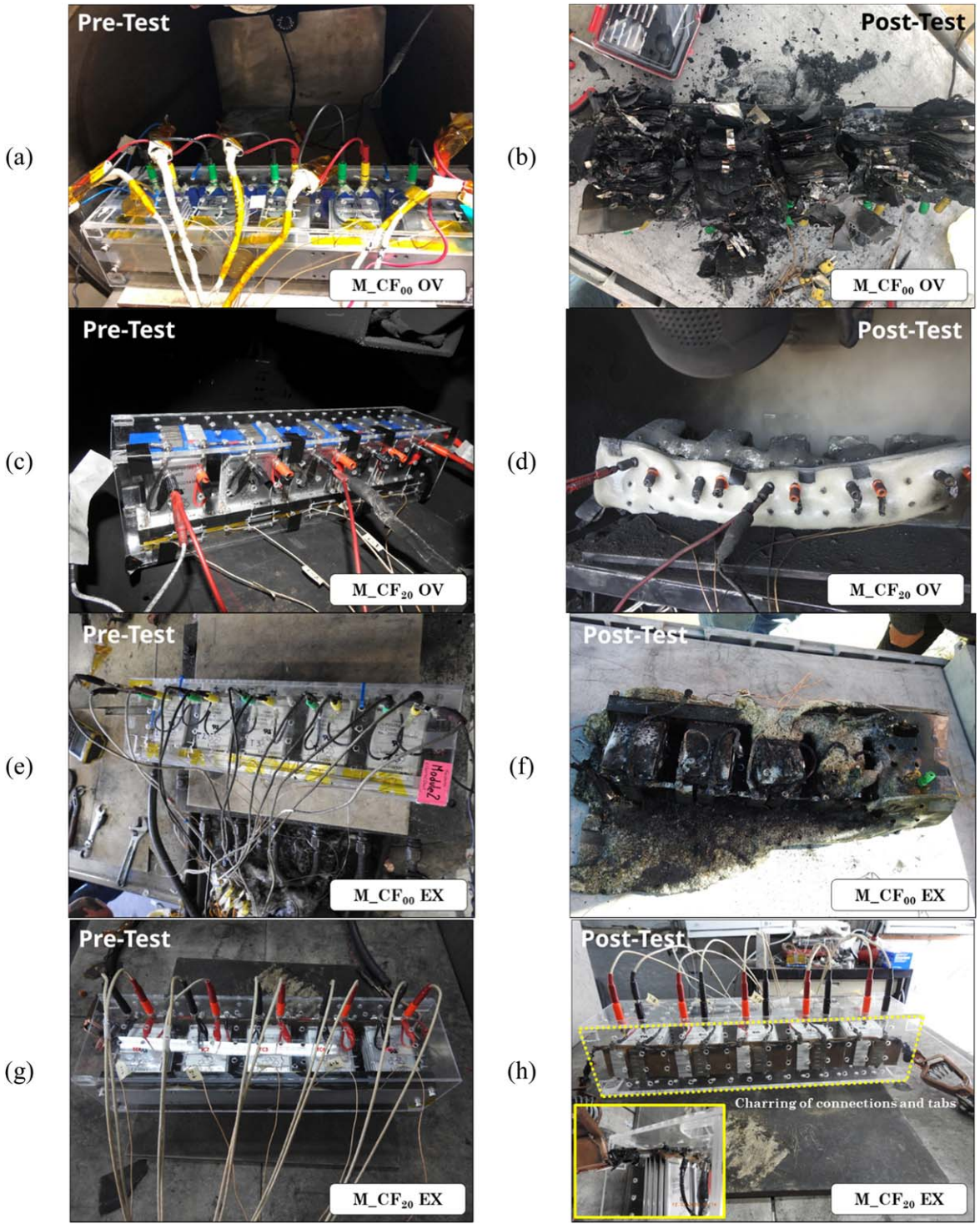

Figure 8. Pre- and post-test photos of the modules subjected to (a)–(d) overcharge at C/3-rate and (e)–(f) external short test. Left column: pre-test photos of modules. Right columns: post-test photos of modules.

the voltage dropped soon after the external resistive load was connected. For the fresh externally shorted module, M_CF$_{00}$ EX, the voltage went from 20.8 V to 3.8 V in less than 2 s. The voltage continued to drop further to 0.0 V after 5 min, see Fig. 9a. At 5 min into the short circuit test, the first bank (Bank 5) went into thermal runaway displaying temperatures greater than 800 °C that caused the voltage to fall to 0 V at the module level. At the beginning of the external short test, the intercell connectors between Banks 1 and 2, the ones closest to the negative terminal of the module, immediately became red hot due to the large current flowing through them. The temperature experienced was so high that it melted the insulation of the connectors between the banks. The voltage of Banks 1 to 4 dropped to zero, and the temperature increased from 23 °C to 465 °C in a few seconds, Figs. 9c and 9d. The elevated temperatures in Banks 1 and 2 caused their cells to vent and go into thermal runaway but no fire was observed. The gases and sparks released subsequently caused Bank 3 and 4 to go into thermal runaway. After 5 min, thermal runaway propagated to Bank 5 and caused one of its cells to go into thermal runaway and catch fire. The maximum temperature measured on Bank 5 was 790 °C, Fig. 9d. Under the

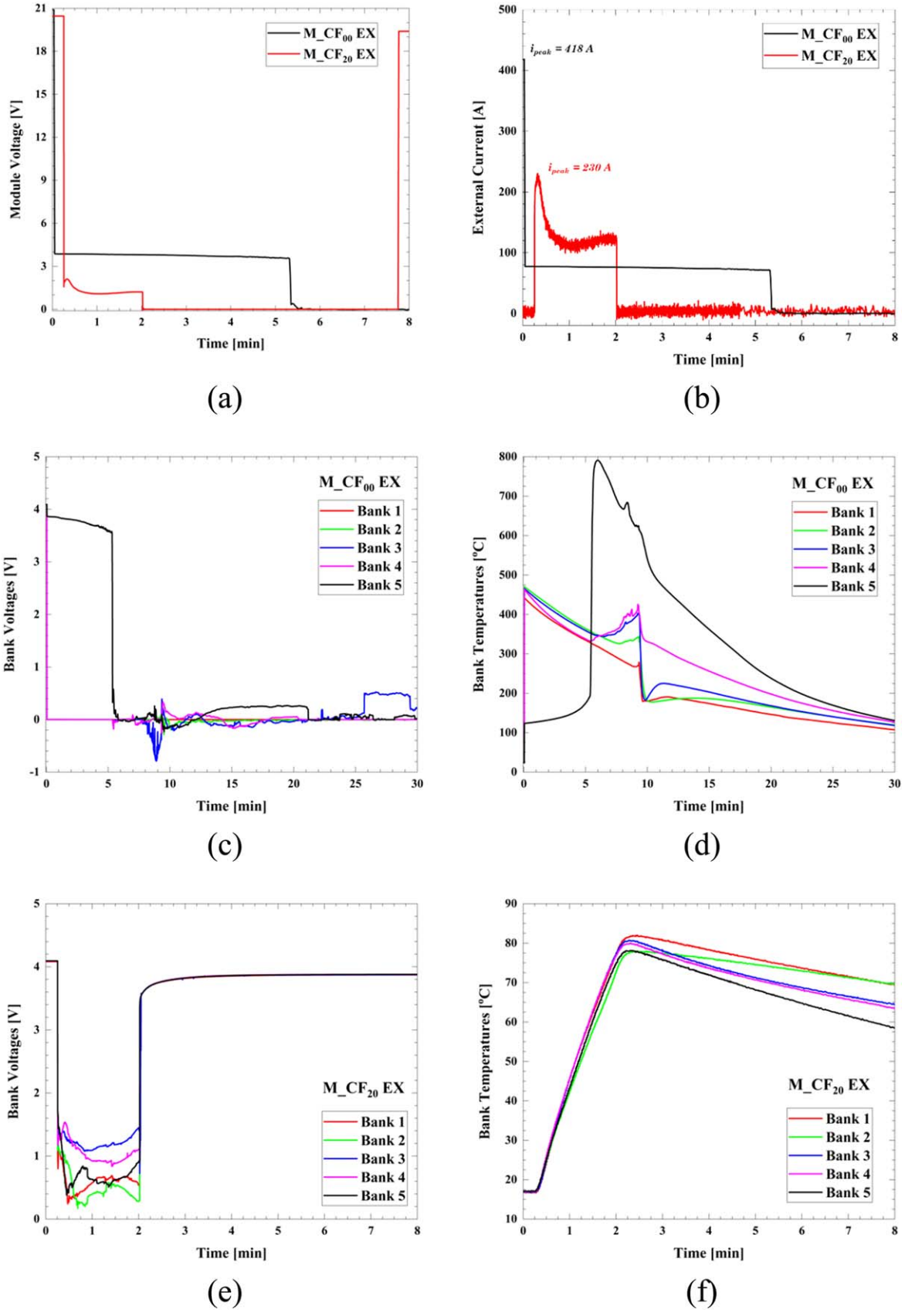

Figure 9. Externally shorted fresh and cycle life aged modules showing (a) module voltages and (b) peak current comparison; fresh module: (c) bank voltages and (d) bank temperatures; cycle life aged module: (e) bank voltages and (f) bank temperatures.

Table II. Summary of external short tests conducted on fresh cells and fresh and aged modules.

ID	Sample	Capacity fade [%]	Cycles	Off-nominal Test	Maximum temperature [°C]	Charring	Swelling	Venting	Thermal runaway	Fire
CF_{00} EX_1	Single Cell	0	0	External Short, 15 mΩ	75	Tabs	Yes	No	No	No
CF_{00} EX_2	Single Cell	0	0	External Short, 15 mΩ	94	Tabs	Yes	No	No	No
CF_{00} EX_3	Single Cell	0	0	External Short, 15 mΩ	94	Tabs	Yes	No	No	No
CF_{00} EX_4	Single Cell	0	0	External Short, 15 mΩ	131	Tabs	No	No	No	No
M_CF_{00} EX	Module	0	0	External Short, 15 mΩ	790	Yes	Yes	Yes	Yes	Yes
M_CF_{20} EX	Module	20	1826	External Short, 15 mΩ	84	Tabs	No	No	No	No

short circuit condition, the peak current recorded was 418 A in the first few milliseconds. Then the current flowing through the external resistive load decreased to approximately 80 A and finally dropped to zero, see Fig. 9b. For the cycle life aged module, M_CF_{20} EX, the voltage went from 20.5 V to 1.7 V in less than 15 s. The voltage continued to drop further for two minutes and then it fell to 0.0 V, see Fig. 9a. The maximum temperature recorded was 80 °C and there was no fire or thermal runaway observed (Fig. 9f). Cells in the banks did display burnt tabs. The peak current recorded was 230 A when the short was applied and then the current decreased to approximately 130 A and finally dropped to zero when the voltage fell to 0.0 V, see Fig. 9b. The voltage of the module dropped to 1.0 V or less for two minutes. It can be observed in Fig. 9e, that once the cell tabs and bank connector got charred, the cell voltages increased again to 3.8 V although the module voltage displayed 0 V due to the burning of the main module connection. This indicates that the cells in the banks were still in good condition and may be cycled again. In terms of the temperature of the banks, the maximum temperature reached was 84 °C in Bank 1, while Bank 2 showed the lowest temperature of 77 °C.

Post-mortem photos for the fresh externally shorted module are provided in Figs. 8e and 8f showing that it went into thermal runaway and was completely charred. Post-mortem photos for the aged externally shorted module revealed that it failed due to the burning of the module connector and charring of the tabs from some of the cells was also observed, Figs. 8g and 8h. The charring of the tabs is consistent with the results observed for the single cells. Burning of the module connector electrically disconnected the module from the external load but the short circuit load transmitted to the cell banks before the connector was fully disconnected caused the cell tabs in some of the banks to char preventing the banks from going into thermal runaway. During the off-nominal test, sparks and a small flame were seen in the area of the connector between the module and the external load, but the flame was not enough to cause a thermal runaway. Thus, none of the cells of the externally shorted aged module exhibited even swelling.

Conclusions

A study on cycle life aging of lithium-ion pouch cells and their behavior under two off-nominal conditions, overcharge and external short, is presented. At the end of the cycle life, none of the single cells and the cells from the modules exhibited swelling. This response indicates that the side reactions induced by cycle life aging is negligible and does not produce a significant amount of gases.

Under high overcharge current condition (1C), fresh cells and aged cells experienced swelling, thermal runaway and fire, whereas cells aged up to 15% capacity experienced swelling and thermal runaway but not fire. Cells with 17%, 18% and 20% CF only experienced swelling and venting of the pouch. According to these results, aging above 15% CF may play a significant role in safety by reducing the amount of active materials available for adverse reaction which signifies a decreased energy content in the cells.

Cells overcharged with a low current (C/3) experienced swelling and venting but did not go into thermal runaway. No additional experiments were conducted on cells with more than 10% CF at this rate of overcharge.

All the overcharged cells exhibited swelling caused by the gases produced at high voltages. The high internal pressure caused by the gases eventually ruptured the pouch and let the gases vent. The rupture size was charge rate dependent, with a larger cell opening in the cells overcharged at the higher rate. The results from the different overcharge currents indicate that the cells have a tolerance to overcharge if the charge current is low and equal to or below 1/3 of the C-rate.

All the shorted fresh cells exhibited charring of the negative tab due to the large current experienced at the imposition of the hard short circuit. The cells exhibited slight to almost no swelling hence cell venting was not observed. The prominent degradation took place in the cathode that exhibited sand-dune-like patterns that may be attributed to drying out, fracture and mechanical degradation due to the high heat produced for a very short time period before the negative tab burns out and disconnects the cell from the load. The sand-dune like patterns may lead to latent failures since this will cause a lack of good contact between the cathode and anode and give rise to deposition of lithium in dendritic form rather than intercalation into the anode.

The modules subjected to an overcharge condition went into thermal runaway and experienced a fire. Both modules reached similar high temperatures once they went into thermal runaway, but the aged module took a longer time to go into thermal runaway. This indicated that although the modules had aged, the cells maintained sufficient energy and electrolyte wetness to cause the catastrophic thermal runaway behavior similar to the fresh cell module.

For the external short condition at the module level, the fresh module went into thermal runaway and got completely burned. Unlike the fresh module, the cycle life aged one did not go into thermal runaway or catch fire. Charring of the cell tabs and module connectors due to large currents that helped prevent the module from going into thermal runaway was observed. The charring of cell tabs has been a safety feature in most pouch cell designs wherein the tab that has the lower melting point melts thus providing protection to the cell itself in a fail-safe mode.

Acknowledgments

Internal research funds from Underwriters Laboratories (UL) were used for this test program and is gratefully acknowledged. Dr. Mukherjee acknowledges financial support from UL for the research carried out at the Energy and Transportation Sciences Lab (ETSL) at Purdue University. Dr. Daniel Juarez-Robles was a Ph.D. student at ETSL under Dr. Mukherjee's guidance at the time this work was carried out. The safety tests were carried out by Saad Azam of Underwriters Laboratories Inc. who is currently a graduate student at Dalhousie University and Dereck J. Lenoir from Johnson Space Center and his team at NASA, Houston, TX. The NASA team is acknowledged for working cohesively with the UL team.

ORCID

Daniel Juarez-Robles https://orcid.org/0000-0003-2746-5775
Judith A. Jeevarajan https://orcid.org/0000-0003-4843-7597

References

1. "Lithium Batteries& Lithium Battery-Powered Devices.." *Federal AviationAdministration, Office of Security and Hazardous Materials Safety*, **2018**, 57 (2018), https://www.faa.gov/about/office_org/headquarters_offices/ash/ash_programs/hazmat/aircarrier_info/.
2. M.-K. Tran and M. Fowler, *Algorithms*, **13**, 1 (2020).
3. S. Abada, G. Marlair, A. Lecocq, M. Petit, V. Sauvant-Moynot, and F. Huet, *J. Power Sources*, **306**, 178 (2016).
4. L. Bravo Diaz, X. He, Z. Hu, F. Restuccia, J. Varela Barreras, M. Marinescu, Y. Patel, G. Offer, and G. Rein, *J. Electrochem. Soc.*, **167**, 090559 (2020).
5. D. Juarez-Robles, J. A. Jeevarajan, and P. P. Mukherjee, *J. Electrochem. Soc.*, **167**, 160510 (2020).
6. D. Juarez-Robles, S. Azam, J. Jeevarajan, and P. P. Mukherjee, *J. Electrochem. Soc.*, **168**, 050535 (2021).
7. C. P. Aiken, J. Self, R. Petibon, X. Xia, J. M. Paulsen, and J. R. Dahn, *J. Electrochem. Soc.*, **162**, A760 (2015).
8. J. Self, C. P. Aiken, R. Petibon, and J. R. Dahn, *J. Electrochem. Soc.*, **162**, A796 (2015).
9. R. Spotnitz and J. Franklin, *J. Power Sources*, **113**, 81 (2003).
10. J. Gale, *Hazardous Materials; Transportation of Lithium Batteries*, **E7-15213**, 44929 (2007), https://www.federalregister.gov/documents/2007/08/09.
11. R. Guo, L. G. Lu, M. G. Ouyang, and X. N. Feng, *Sci. Rep.*, **6**, 1 (2016).
12. F. Larsson and B. E. Mellander, *J. Electrochem. Soc.*, **161**, A1611 (2014).
13. M.-S. Wu, P.-C. J. Chiang, J.-C. Lin, and Y.-S. Jan, *Electrochim. Acta*, **49**, 1803 (2004).
14. C. Wu, J. L. Sun, C. B. Zhu, Y. W. Ge, and Y. P. Zhao, "Research on Overcharge and Overdischarge of Lithium-ion Batteries." *IEEE Vehicle Power*, **-**, -ISI>://WOS:000377904400133978-1-4673-7637-2/15/2015 ISBN 1938-8756.
15. M. G. Ouyang, D. S. Ren, L. G. Lu, J. Q. Li, X. N. Feng, X. B. Han, and G. M. Liu, *J. Power Sources*, **279**, 626 (2015).

16. D. Juarez-Robles, A. A. Vyas, C. Fear, J. A. Jeevarajan, and P. P. Mukherjee, *J. Electrochem. Soc.*, **167**, 090547 (2020).
17. D. J. Xiong, R. Petibon, M. Nie, L. Ma, J. Xia, and J. R. Dahn, *J. Electrochem. Soc.*, **163**, A546 (2016).
18. D. P. S. Finegan, Mario, B. Robinson, James, T. Bernhard, D. M. Marco, H. Gareth, J. L. Brett, Dan, and R.;. Shearing, Paul, *Phys. Chem. Chem. Phys.*, **18**, 30912 (2016).
19. C. Essl, A. W. Golubkov, and A. Fuchs, *J. Electrochem. Soc.*, **167**, 130542 (2020).
20. L. Sun, C. Wei, D. Guo, J. Liu, Z. Zhao, Z. Zheng, and Y. Jin, *Fire Technol.*, **56**, 1555 (2020).
21. D. Ren, X. Feng, L. Lu, X. He, and M. Ouyang, *Appl Energ*, **250**, 323 (2019).
22. A. W. Golubkov, S. Scheikl, R. Planteu, G. Voitic, H. Wiltsche, C. Stangl, G. Fauler, A. Thaler, and V. Hacker, *RSC Adv.*, **5**, 57171 (2015).
23. L. Geng, D. L. Wood, S. A. Lewis, R. M. Connatser, M. Li, C. J. Jafta, and I. Belharouak, *J. Power Sources*, **466**, 228211 (2020).
24. S. Klein, P. Bärmann, T. Beuse, K. Borzutzki, J. Frerichs, J. Kasnatscheew, M. Winter, and T. Placke, *Chem.Sus.Chem.*, **14**(2), 595 (2020).
25. C. F. Lopez, J. A. Jeevarajan, and P. P. Mukherjee, *J. Electrochem. Soc.*, **162**(9), A1905 (2015).
26. X.-G. Yang, Y. Leng, G. Zhang, S. Ge, and C.-Y. Wang, *J. Power Sources*, **360**, 28 (2017).
27. Y. Preger, H. M. Barkholtz, A. Fresquez, D. L. Campbell, B. W. Juba, J. Romàn-Kustas, S. R. Ferreira, and B. Chalamala, *J. Electrochem. Soc.*, **167**, 120532 (2020).